Sensor-Failure Detection Method for Flexible Structures

H. Baruh* and K. Choe†
Rutgers University, New Brunswick, New Jersey

A method is presented for the identification of sensor failures in distributed structures. The procedure can be used with controlled or uncontrolled systems, and is applicable when a large number of sensors are used. For control systems, the failure detection can be implemented with any control scheme. It makes use of estimates of the system state to identify the faulty sensor(s). The sensors output is estimated using modal analysis and a decentralized approach. These estimates are plotted and compared with plots of the actual sensors measurements to detect failure. A sequential decision-making sequence for failure detection is proposed.

I. Introduction

A CRITICAL problem in the analysis and control of structures and other distributed-parameter systems is the reliability of the components that monitor their behavior and control the motion. Failure of such components either gives incorrect information or it causes erroneous inputs to be applied, thus degrading the analysis and overall performance. Sometimes, a faulty component can lead to instabilities. It is important that immediately after failure the faulty components be identified and corrective action taken.

This paper is concerned with the identification of sensor failures in flexible structures and distributed-parameter systems. The sensors can be used to monitor the behavior of the distributed system, or as part of a feedback control process. The failure detection is based on estimating the sensors output, and then comparing these estimates with the actual sensors measurements.

What makes failure detection in large structures and other high-order dynamical systems complicated is the necessity to use a large number of components to monitor and control the system behavior adequately. Most of the work related to the detection and identification of component failure has been performed for low-order systems where a small number of components are used.[1-4] In such cases, the system hardware is also used to detect failure. Surveys of existing fault detection algorithms can be found in Refs. 5 and 6. Among the common methods used are the generalized likelihood ratio or maximum likelihood ratio methods. The effects of factors that affect the reliability of the failure detection, such as uncertainties in the system model and measurement error, have been analyzed in Refs. 7-10.

The problem of failure detection for flexible structures and high-order systems has recently begun to receive more interest.[11-16] Functional redundancy has been used for nuclear reactors,[11] where more than one observer is designed to estimate the same parameters. VanderVelde[12] outlines failure detection schemes that are applicable to flexible spacecraft. Among failure detection methods are voting, filtering, and parity relations. Parity relations make use of redundancies in the system so that, under normal circumstances, they should be equal to zero. In the event of failure, these relations no longer equal zero, indicating failure. The problem of placement of control system components from a reliability standpoint was considered by VanderVelde and Carignan[13] and Montgomery.[14] Actuator failure detection in distributed-parameter systems was considered by Baruh.[16]

In this paper, the sensors output and magnitude of the external excitation at a certain instant are used to generate estimates of the sensors measurements at the next sampling time. These estimates are then compared with the actual measurements to detect failure. The effects of model truncation, unknown external disturbances, and measurement noise are also investigated. The method for failure detection described herein is envisioned as part of a sequential decision tree to detect failure, in which the system hardware and software will be used together.

II. System Equations

A large number of dynamical systems can be modeled mathematically as distributed-parameter systems. Among these are large flexible structures, chemical processes, and thermal systems. The class of distributed systems considered here are[17]

$$m(x)\ddot{u}(x,t) + Lu(x,t) = f(x,t) \tag{1}$$

where $u(x,t)$ is the displacement at spatial coordinate x at time t, $m(x)$ is a weighting function (representing the mass distribution for structures), L a linear differential self-adjoint operator (denoting the stiffness for structures), and $f(x,t)$ the external excitation, including control.

It follows that the system of Eq. (1) admits an infinite and countable set of non-negative eigenvalues, related to the natural frequencies by $\lambda_r = \omega_r^2$ $(r=1,2,\ldots)$, and corresponding eigenfunctions $\phi_r(x)$ $(r=1,2,\ldots)$. The eigenfunctions are mutually orthogonal and can be normalized to yield $\langle \phi_r(x), m(x)\phi_s(x)\rangle = \delta_{rs}$, $\langle \phi_r(x), L\phi_s(x)\rangle = \lambda_r\delta_{rs}$, $(r,s=1,2,\ldots)$ where δ_{rs} is the Kronecker delta.

The displacement $u(x,t)$ and input $f(x,t)$ can be expanded as

$$u(x,t) = \sum_{r=1}^{\infty} \phi_r(x)u_r(t) \tag{2a}$$

$$f(x,t) = \sum_{r=1}^{\infty} m(x)\phi_r(x)f_r(t) \tag{2b}$$

where $u_r(t)$ and $f_r(t)$ are modal coordinates and modal forces, respectively. Using Eqs. (2) and the orthogonality relations we obtain

$$u_r(t) = \langle u(x,t), m(x)\phi_r(x)\rangle \tag{3a}$$

$$f_r(t) = \langle f(x,t), \phi_r(x)\rangle \tag{3b}$$

Received April 7, 1986; revision received Oct. 31, 1986. Copyright © American Institute of Aeronautics and Astronautics, Inc., 1987. All rights reserved.

*Assistant Professor, Department of Mechanical and Aerospace Engineering. Refs. 7-10.

†Graduate Assistant, Department of Mechanical and Aerospace Engineering.

Equations (2) and (3) constitute the so-called expansion theorem, leading to the modal equations of motion

$$\ddot{u}_r(t)+\omega_r^2 u_r(t)=f_r(t), \qquad r=1,2,\ldots \tag{4}$$

For control systems, most methods use the displacement and velocity of the structure as feedback, so that

$$f(x,t)=f[u(x,t),\dot{u}(x,t)] \tag{5}$$

Considering implementation by discrete components, Eq. (5) becomes

$$F(t)=F[y(t),\dot{y}(t)] \tag{6}$$

where

$$F(t)=[F_1(t)F_2(t)\ldots F_m(t)]^T,$$

$$y(t)=[u(x_1,t)u(x_2,t)\ldots \mu(x_p,t)]^T \tag{7}$$

denote the external forces and sensors measurements, respectively, where m is the number of force inputs and p the number of sensors.

III. Effects of Sensor Failure

We consider the following model to describe sensor failure. The actual measured system output, denoted by $y_F(t)$, is defined as

$$y_F(t)=Sy(t)+v(t)+q(t) \tag{8}$$

where S is a diagonal matrix having the form $S=\operatorname{diag}[S_1S_2\ldots S_p]$ and $S_j\,(j=1,2,\ldots,p)$ is a parameter denoting the level of failure in the jth sensor. Note that $S_j\,(j=1,2,\ldots,p)$ can be time varying as well. The erratic behavior and noise in each sensor are denoted by $v(t)$ and $q(t)$, respectively. Generally, these vectors are assumed to be random variables.

In some control approaches, one needs to extract part of the modal coordinates from the system output. Here, we wish to examine the effects of sensor failure on this process. We first consider Luenberger observers, which are described by the equation

$$\dot{\hat{x}}(t)=A\hat{x}(t)+B'F(t)+K[y(t)-\hat{y}(t)] \tag{9}$$

where $\hat{x}(t)$ is the estimate of the state vector $x(t)$, and A and B' are matrices that describe the motion in the state space by the relations

$$\dot{x}(t)=Ax(t)+B'F(t), \quad y(t)=Dx(t) \tag{10}$$

where A is the state matrix and B' is dependent on the locations of the external disturbances. $\hat{y}(t)$ is the estimate of the output $y(t)$ in the form

$$\hat{y}(t)=D\hat{x}(t) \tag{11}$$

and entries of D depend on the kind and location of the sensors. K is the observer gain matrix. The state vector $x(t)$ is generally chosen as $x(t)=[u_1,\dot{u}_1,u_2,\dot{u}_2,\ldots,u_n,\dot{u}_n]^T$, where n is the number of controlled or monitored modes retained in the model. The consequences of using an observer of finite order to control a distributed system are considered by Balas[18] and are shown to lead to observation spillover, which may have undesirable effects.

Defining by $e(t)$ the error in the observation process and assuming a linear control law in the form $F(t)=G\hat{x}(t)$, the observer equations become

$$\begin{bmatrix}\dot{x}(t)\\ \dot{e}(t)\end{bmatrix}=\begin{bmatrix}A+BG & -BG\\ 0 & A-KD\end{bmatrix}\begin{bmatrix}x(t)\\ e(t)\end{bmatrix} \tag{12}$$

In the event of sensor failure, the output vector $y(t)$ in Eq. (9) is replaced by the actual measurement vector $y_F(t)$. Equation (12) then yields

$$\begin{bmatrix}\dot{x}(t)\\ \dot{e}(t)\end{bmatrix}=\begin{bmatrix}A+BG & -BG\\ K(1-S)D & A-KD\end{bmatrix}\begin{bmatrix}x(t)\\ e(t)\end{bmatrix}-\begin{bmatrix}0\\ K[v(t)+q(t)]\end{bmatrix} \tag{13}$$

Clearly, failure affects both the observer and system closed-loop poles. The deterministic separation principle is no longer valid, so a rational assessment of the closed-loop system and observer poles becomes difficult.

When modal filters are used, the sensors output is interpolated to obtain a spatially continuous estimate $\bar{u}(x,t)$ of the distributed profile $u(x,t)$. This estimate is then used in conjunction with Eq. (3a) to yield estimates of the modal coordinates.[17] We select an interpolation process where the time and space dependency are separate,[19] so that

$$\bar{u}(x,t)=\sum_{j=1}^{p}C(x,x_j)u(x_j,t) \tag{14}$$

where $C(x,x_j)$ are interpolation functions and x_j denote the sensors locations. A similar equation can be written for velocity measurements. Introducing Eq. (14) into Eq. (3a) we obtain estimates of the modal coordinates in the form

$$\bar{u}_r(t)=\langle\bar{u}(x,t),m(x)\phi_r(x)\rangle=\sum_{j=1}^{p}C_{rj}y_j(t) \tag{15}$$

where

$$C_{rj}=\langle C(x,x_j),m(x)\phi_r(x)\rangle, \quad r=1,2,\ldots;\ j=1,2,\ldots,p \tag{16}$$

are modal filter gains and can be computed off-line. It can be shown that the estimation error[19] has the form

$$e(t)=u(t)-\bar{u}(t)=[1-CD]u(t) \tag{17}$$

where

$$e(t)=[e_1(t)e_2(t)\ldots]^T, \quad u(t)=[u_1(t)u_2(t)\ldots]^T \tag{18}$$

and $e_r(t)=u_r(t)-\bar{u}_r(t)$, $(r=1,2,\ldots)$. D is defined such that $D_{jr}=\phi_r(x_j)$, and

$$y(t)=Du(t) \tag{19}$$

Another way of implementing modal filters is to truncate the number of monitored modes at p. In this case, D becomes a square matrix, and if the sensors locations are chosen such that D is nonsingular, the modal coordinates can be estimated by inverting Eq. (19) or, $u(t)=D^{-1}y(t)$. Note that the error $e(t)$ vector used for modal filters and matrix D are different than the ones used for Luenberger observers. It should also be noted that implementation of modal filters does not require any knowledge about external excitations. Introducing the actual measurement vector $y_F(t)$ into Eq. (17), the error vector becomes

$$e(t)=[1-CSD]u(t)-C[v(t)+q(t)] \tag{20}$$

A control method that does not make use of modal coordinates is colocated control, for which the control law has the form $F(t) = G\dot{y}(t)$, where G is a diagonal matrix of the form $G = \text{diag}\ (G_1 G_2 \ldots G_m)$.[20] When a sensor fails, only the command going into the actuator colocated with the faulty sensor changes. Depending on the type of failure, the control system may or may not be destabilized.

We observe from the above that failure of a sensor affects all the closed-loop poles. One can intuitively expect that as the number of sensors is increased, the consequences of sensor failure become less critical. On the other hand, increasing the number of sensors also increases the probabilities of failure. These factors need to be weighed against each other.

IV. Failure Detection

The sensor failure detection scheme proposed herein is based on monitoring the behavior of each sensor, and can be implemented whether the distributed system is controlled or not. The system output is measured at sampling instances $t = kT\ (k = 1,2,\ldots)$, where T is the sampling period. After each measurement, estimates of the sensors measurements at subsequent time instances are generated. These estimates are then compared with the actual measurements to detect failure.

We will use modal analysis to obtain estimates of the response $y(t)$ and $\dot{y}(t)$ at the end of each sampling period. To this end, we need to extract the modal coordinates and forces. The modal forces can be obtained from the external excitation using Eq. (3b)[17]

$$f_r(t) = \sum_{j=1}^{m} \phi_r(x_j^a) F_j(t), \qquad r = 1,2,\ldots \tag{21}$$

where $x_j^a\ (j = 1,2,\ldots,m)$ denote the actuators locations or locations of other external inputs. The locations of disturbances are generally not known.

Given $u_r(kT)$ and $\dot{u}_r(kT)\ (l = 1,2,\ldots)$ and assuming that the modal input $f_r(kT)$ remains constant for the duration of the sampling period, the system response at the next sampling instant becomes

$$u_r(kT+T) = u_r(kT)\cos\omega_r T + \dot{u}_r(kT)\sin(\omega_r T)/\omega_r + f_r(kT)(1-\cos\omega_r T)/\omega_r^2 \tag{22a}$$

$$\dot{u}_r(kT+T) = -u_r(kT)\omega_r\sin\omega_r T + \dot{u}_r(kT)\cos\omega_r T + f_r(kT)\sin(\omega_r T)/\omega_r \tag{22b}$$

Using Eqs. (22a) and (22b) we can write the following for velocity sensors:

$$\dot{y}_j(kT+T) = \sum_{r=1}^{\infty} \phi_r(x_j)\dot{u}_r(kT+T), \quad j = 1,2,\ldots,p \tag{23}$$

where x_j denote the sensors locations. Using a finite number of sensors it is impossible to extract from the system output, monitor, and control all the modes accurately. In general, one monitors a finite number of modes, which are, for control systems, the controlled modes and sometimes a few of the uncontrolled modes. Denoting by ℓ the number of monitored modes, Eq. (23) becomes

$$\hat{\dot{y}}_j(kT+T) = \sum_{r=1}^{\ell} \phi_r(x_j)\hat{\dot{u}}_r(kT+T), \qquad j = 1,2,\ldots,p \tag{24}$$

where $\hat{\dot{y}}_j(kT+T)$ is the estimate of the velocity $\dot{y}_j(kT+T)$ of the jth sensor. The estimates $\hat{u}_r(kT+T)$ and $\hat{\dot{u}}_r(kT+T)$ of the modal coordinates and velocities $u_r(kT+T)$ and $\dot{u}_r(kT+T)$, can be generated using Eqs. (22) as

$$\hat{u}_r(kT+T) = \bar{u}_r(kT)\cos\omega_r T + \bar{\dot{u}}_r(kT)\sin(\omega_r T)/\omega_r + f_r(kT)(1-\cos\omega_r T)/\omega_r^2$$

$$\hat{\dot{u}}_r(kT+T) = -\bar{u}_r(kT)\omega_r\sin\omega_r T + \bar{\dot{u}}_r(kT)\cos\omega_r T + f_r(kT)\sin(\omega_r T)/\omega_r \tag{25}$$

where the bars over $\bar{u}_r(kT)$ and $\bar{\dot{u}}_r(kT)$ denote that these quantities are extracted from the system output using a state reconstruction mechanism, such as a modal filter or Luenberger observer. These estimates, $\hat{u}_r(kT+T)$ and $\hat{\dot{u}}_r(kT+T)\ (r = 1,2,\ldots,\ell)$, are affected by measurement noise and by errors in the extraction of $\bar{u}_r(kT)$ and $\bar{\dot{u}}_r(kT)$ from the system output. In addition, estimates of the actual displacements and velocities at the sensors locations are generated using a finite number of modes. Because the unmodeled modes are more wrinkled and have lower amplitudes, estimates of the sensors measurments obtained by Eq. (24) will have amplitudes similar to the actual sensors measurements, but will be smoother.

The contribution of the faulty sensor in the state reconstruction process is to contaminate all the modal coordinates, which subsequntly affects the estimates of all the sensors' outputs. Intuitively, one expects the estimates of sensors close to the faulty one to be more affected.

We note from Eqs. (24) and (25) that both modal displacements and velocities are required to obtain estimates of the system output at the sensors locations. Whereas an observer can generate both modal displacements and velocities from a single set of measurements, separate sets of displacement and velocity measurments are required to implement modal filters. We also observe that failure of a displacement sensor affects the failure detection in a velocity sensor and vice versa when Eqs. (24) and (25) are used. To avoid this, and to accommodate cases when modal filters are used, we wish to develop relationships that estimate modal velocities (displacements) from previously computed modal velocities (displacements) alone. From Eq. (22b) we express $u_r(kT)$ as

$$u_r(kT) = -\dot{u}_r(kT+T)/(\omega_r\sin\omega_r T) + \dot{u}_r(kT)\cos\omega_r T/(\omega_r\sin\omega_r T) + f_r(kT)/\omega_r^2 \tag{26}$$

Substitution of Eq. (26) into Eq. (22a) yields

$$u_r(kT+T) = -\dot{u}_r(kT+T)\cos\omega_r T/(\omega_r\sin\omega_r T) + \dot{u}_r(kT)/(\omega_r\sin\omega_r T) + f_r(kT)/\omega_r^2 \tag{27}$$

Changing the time from kT to $kT+T$ in Eq. (22b) we obtain for $\dot{u}_r(kT+T)$

$$\dot{u}_r(kT+2T) = -u_r(kT+T)\omega_r\sin\omega_r T + \dot{u}_r(kT+T)\cos\omega_r T + f_r(kT+T)\sin(\omega_r T)/\omega_r \tag{28}$$

Substituting Eq. (27) into Eq. (28) and rearranging we arrive at

$$\dot{u}_r(kT+2T) = 2\dot{u}_r(kT+T)\cos\omega_r T - \dot{u}_r(t) + [f_r(kT+T) - f_r(kT)]\sin(\omega_r T)/\omega_r \tag{29}$$

which does not contain any modal displacement expressions and can be used to estimate $\dot{u}_r(kT+2T)$ given previous modal velocities. Using Eqs. (24) and (29), we can write

$$\hat{\dot{y}}_j(kT+2T) = \sum_{r=1}^{\ell} \phi_r(x_j)\hat{\dot{u}}_r(kT+2T),$$

$$j=1,2,\ldots,p; \quad k=0,1,2,\ldots \tag{30a}$$

$$\hat{\dot{u}}_r(kT+2T) = 2\bar{\dot{u}}_r(kT+T)\cos\omega_r T - \bar{\dot{u}}_r(kT)$$
$$+ [f_r(kT+T) - f_r(kT)]\sin(\omega_r T)/\omega_r \quad r=1,2,\ldots,\ell \tag{30b}$$

Noting that ideally the upper limit of the summation would be infinity, Eqs. (30) can be rewritten as

$$\hat{\dot{y}}_j(kT+2T) = -\dot{y}_j(kT) + \sum_{r=1}^{\ell} \phi_r(x_j)\{2\bar{\dot{u}}_r(kT+T)\cos\omega_r T$$
$$+ [f_r(kT+T) - f_r(kT)]\sin(\omega_r T/\omega_r)\} \tag{31}$$

Because we assume that a finite number of modes (ℓ) contribute to the response of the structure significantly, and that this number is known relatively accurately, the sampling period T can be chosen such that $\omega_r T (r=1,2,\ldots,\ell)$ are small. This permits use of the small angles assumption. Introducing the approximations $\cos\omega_r T \approx 1$, $\sin\omega_r T \approx \omega_r T$ $(r=1,2,\ldots,\ell)$ and assuming that the modes that are not monitored can be ignored, Eq. (31) can further be approximated as

$$\hat{\dot{y}}_j(kT+2T) = 2\dot{y}_j(kT+T) - \dot{y}_j(kT)$$
$$+ T\sum_{r=1}^{\ell} \phi_r(x_j)[f_r(kT+T) - f_r(kT)] \tag{32}$$

A special case exists when the external excitations can be assumed as constant for two sampling periods. For control systems, this can be regarded as having a control sample of twice the length as the measurement sample. Using this assumption and setting $f_r(kT+T) = f_r(kT)$ $(k=0,2,4,\ldots;$ $r=1,2,\ldots)$ in Eqs. (30)-(32) yields

$$\hat{\dot{y}}_j(2kT) = \sum_{r=1}^{\ell} \phi_r(x_j)\{2\bar{\dot{u}}_r(2kT-T)\cos\omega_r T$$
$$- \bar{\dot{u}}_r[2(k-1)T]\} \tag{33a}$$

$$\hat{\dot{y}}_j(2kT) = 2\sum_{r=1}^{\ell} \phi_r(x_j)\bar{\dot{u}}_r(2kT-T)\cos\omega_r T$$
$$- \dot{y}_j[2(k-1)\mathrm{T}], \tag{33b}$$

$$\hat{\dot{y}}_j(2kT) = 2\dot{y}_j(2kT-T) - \dot{y}_j[2(k-1)T] \tag{33c}$$

$k=1,2,\ldots;\ j=1,2,\ldots,p$

We note that by using Eqs. (33), the sensor failure detection becomes independent of the nature of the external excitation. For cases where the external excitation is not accurately known one can still check for faulty sensors. For control systems, Eqs. (33) permit a sensor failure detection independent of the actuator magnitudes, and of any possible actuator failure, assuming that the faulty actuator generates the same erroneous signal during two sampling periods. It should be noted that the noise associated with the actuators input will not remain the same for two sampling periods. However, system simulations indicate that the effect of such noise and of the actuator's signals or other inputs not being constant over two sampling periods is minimal.

We note that Eqs. (33a) and (33b) estimate the jth sensor's output using all the sensors measurements, and Eq. (33c) estimates the jth sensor's output using the jth sensor alone. To further verify failure, it is desirable to also estimate the output of the jth sensor without using measurement of the jth sensor at all. To this end, we first consider estimation of the velocities at the sensors locations by interpolation of the outputs of nearby sensors. To this end, a wide variety of interpolation methods can be used (e.g., Ref. 21). Also, for sensors at the boundaries, outputs of nearby sensors can be extrapolated, so that we can write

$$\dot{y}_j^i(kT) = G[\dot{y}_{j+1}(kT), \dot{y}_{j-1}(kT), \dot{y}_{j+2}(kT), \ldots] \tag{34}$$

where G is an interpolation (or extrapolation) function and $\dot{y}_j^i(kT)$ is the interpolated estimate of $\dot{y}_j(kT)$.

Another way of not using $\dot{y}_j(t)$ to estimate $\dot{y}_j(t)$ is as follows. In general, the matrix D is of order $px\infty$. If we decide to monitor p modes ($\ell=p$), D becomes a square matrix, and if the sensors are placed such that D is nonsingular, we can write

$$\dot{u}(t) = D^{-1}\dot{y}(t) \tag{35}$$

where $\dot{u}(t)$ is now of order p. To monitor these modes without the jth sensor, we truncate $\dot{u}(t)$ and $\dot{y}(t)$ to order $p-1$ as

$$\dot{u}'(t) = [\dot{u}_1(t)\dot{u}_2(t)\ldots\dot{u}_{p-1}(t)]^T$$
$$\dot{y}'(t) = [\dot{y}_1(t)\dot{y}_2(t)\ldots\dot{y}_{j-1}(t)\dot{y}_{j+1}(t)\ldots\dot{y}_p(t)]^T \tag{36}$$

By striking out the jth row and nth column from D, we obtain D', so that we can now write

$$\dot{u}'(t) = (D')^{-1}\dot{y}'(t) \tag{37}$$

It may appear that to estimate the outputs of p sensors, inversions of matrices of order $(p-1)\,x(p-1)$ need to be computed. However, because D^{-1} is known, the matrix inversion process can be shortened. Partitioning D and D^{-1} into

$$D = \begin{bmatrix} D_{11} & D_{12} \\ D_{21} & D_{22} \\ D_{31} & D_{32} \end{bmatrix} \quad D^{-1} = \begin{bmatrix} e_{11} & e_{12} & e_{13} \\ e_{21} & e_{22} & e_{23} \end{bmatrix} \tag{38}$$

where D_{21} and D_{22} constitute the jth row of D, $(D')^{-1}$ can be calculated as

$$(D')^{-1} = \begin{bmatrix} D_{11} \\ D_1 \end{bmatrix}^{-1} = [[e_{11}3e_{13}] - e_{12}e_{22}^{-1}[e_{21} | e_{23}]] \tag{39}$$

It can be easily shown that if D is nonsingular, so is D'.

The relations developed above can be used to detect velocity sensor failure. For acceleration sensors we can manipulate Eqs. (22) and write a recursive relation in terms of the modal accelerations as[16]

$$\ddot{u}_r(kT+3T) = 2\ddot{u}_r(kT+2T)\cos\omega_r T - \ddot{u}_r(kT+T)$$
$$+ f_r(kT+2T) - f_r(kT) \tag{40}$$

Equation (40) is valid when $f_r(kT+T) = f_r(kT)$. It follows that acceleration sensor failure can be detected by using modal accelerations only, which, when modal filters are used, require only acceleration measurements.

V. A Sequential Decision-making Scheme

A problem that exists during failure detection is the reliability of the relations used to estimate the sensors output. In addition to inaccuracies associated with modeling errors, measurement and actuator noise, actuator failure, and generation of the modal coordinates, one must also be concerned with the effect of failure of one sensor on the failure detection of another sensor. Also, when using Eq. (33c), some forms of failure cannot be detected, especially when the level of failure remains the same and because Eq. (33c) is insensitive to bias offset. In order to increase the reliability level of the failure detection, and to utilize fully all information obtained from the measurements, we develop a sequential decision tree. The process, described here for velocity sensors, can be extended to displacement or acceleration sensors, and consists of the following steps:

1) When any one of the estimates of the system output generated by Eqs. (30–35) does not agree with the actual measurements, begin to look for failure. If the jth sensor is faulty, estimates of some of the nearby sensors are possibly affected.

2) Based on the number and type of estimates that do not agree with the actual measurements, identify a suspect sensor as faulty (say jth). To this end, guidelines are proposed by Choe.[23] Extract the modal coordinates from the system output using the estimate of $\dot{y}_j(kT)$, obtained by interpolation [Eq. (34)], instead of the actual measurement of $\dot{y}_j(kT)$. Or extract the modal coordinates from the system output by using Eq. (37). (Note that this part of the failure detection can be performed as an off-line operation if the past history of the system output is also considered.)

If by eliminating the contribution of $\dot{y}_j(t)$ estimates of the outputs of the other sensors (that were considered as possibly faulty) match their actual measurements, and the estimate of the suspect sensor changes and becomes even more different than the sensors measurement, conclude that the jth sensor is the faulty one. If the estimates of nearby and other sensors do not improve or get worse, the jth sensor is not faulty. Then, identify another sensor as possibly faulty and eliminate its contribution from the system response.

3) When detecting failure, estimates of the modal coordinates are generated first. Then, the velocities at the sensors locations are identified. The estimates of the modal coordinates are not compared with the modal coordinates extracted from the system output. In the event of failure, all the modal coordinates are affected. It follows that comparing the estimated and extracted modal coordinates alone indicates failure, but does not identify a faulty sensor. On the other hand, if a sensor (say jth) is placed on one of the nodes or nodal lines of a certain mode, say the rth one, then failure of that sensor will not affect the extraction of $\dot{u}_r(t)$ from the system output, at least when modal filters are used. This property can be utilized to help verify failure, and it provides a guideline for sensor placement (to place each sensor on one of the nodes or nodal lines of a monitored mode). It should also be noted that the system hardware also gives some information regarding faulty sensors, and that this information should be used in conjunction with the analysis previously described to verify failure further.

VI. Illustrative Example

As an illustrative example, we consider sensor failure detection during control of the transverse vibration of a uniform beam pinned at both ends. The mass and stiffness distributions of the beam are $m(x)=1$, $EI(x)=1$, $0<x<a$, where a is the length of the beam, taken as $a=10$. The stiffness operator has the form $L=EI\,\mathrm{d}^4/\mathrm{d}x^4$. The associated eigensolution is[17]

$$\lambda_r=\omega_r^2=(r\pi/a)^4,\qquad \phi_r(x)=\sqrt{2/a}\,\sin(r\pi x/a),\qquad r=1,2,\ldots \tag{41}$$

We assume that the first 15 modes contribute to the system response and design a control system that suppresses the motion of the lowest four modes using four actuators. The sensors output is processed using modal filters. Details of the modal filter design may be found in Ref. 19. The control law is based on natural control.[22]

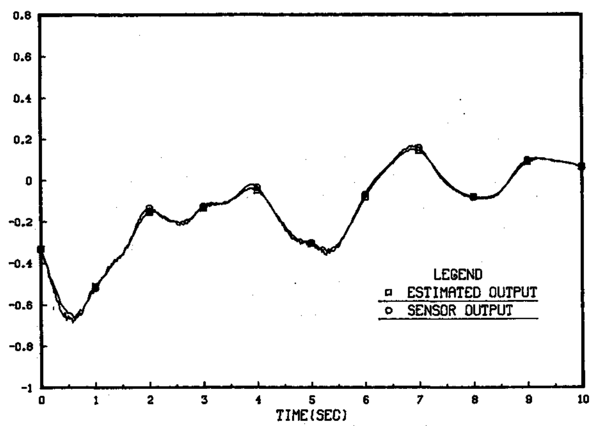

Fig. 1 Estimate of the 6th sensor (no failure).

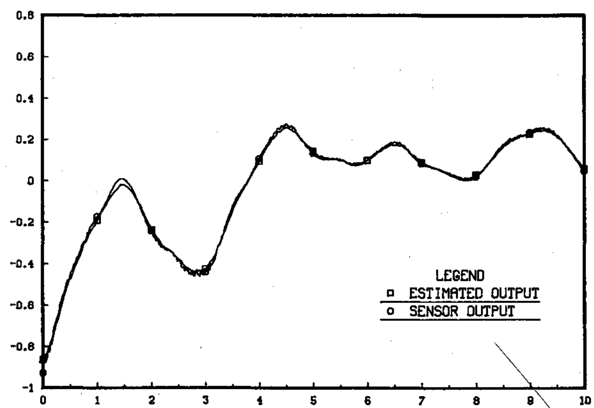

Fig. 2 Estimate of the 8th sensor (no failure).

Table 1 The *CD* matrix for 11 sensors

0.9999	0.0000	0.0000	0.0000	0.0000	0.0000	0.0000	0.0000
0.0000	0.9988	0.0000	0.0000	0.0000	0.0000	0.0000	0.0000
0.0000	0.0000	0.9940	0.0000	0.0000	0.0000	0.0000	0.0000
0.0000	0.0000	0.0000	0.9821	0.0000	0.0000	0.0000	0.2106

Table 2 *CSD* matrix for 11 sensors

0.9858	−0.0244	−0.0282	−0.0244	−0.0141	0.0000	0.0141	0.0244
−0.0253	0.9550	−0.0505	−0.0438	−0.0253	0.0000	0.0253	0.0438
−0.0306	−0.0531	0.9328	−0.0531	−0.0306	0.0000	0.0306	0.0531
−0.0278	−0.0482	−0.0557	0.9339	0.0278	0.0000	−0.0278	0.2588

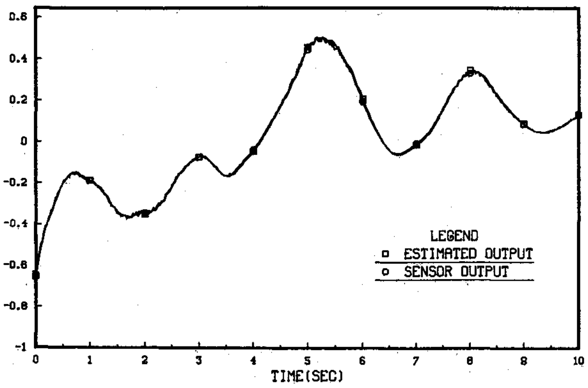

Fig. 3 Estimate of the 9th sensor (no failure).

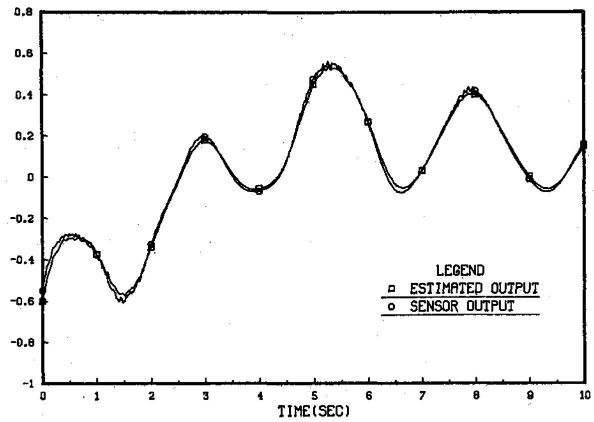

Fig. 4 Estimate of the 10th sensor (no failure).

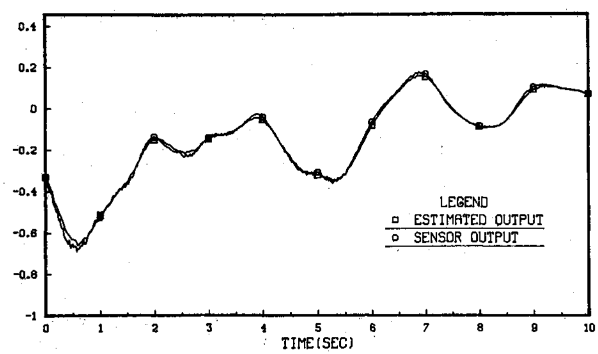

Fig. 5 Estimate of 6th sensor (9th sensor fails, no corrective action).

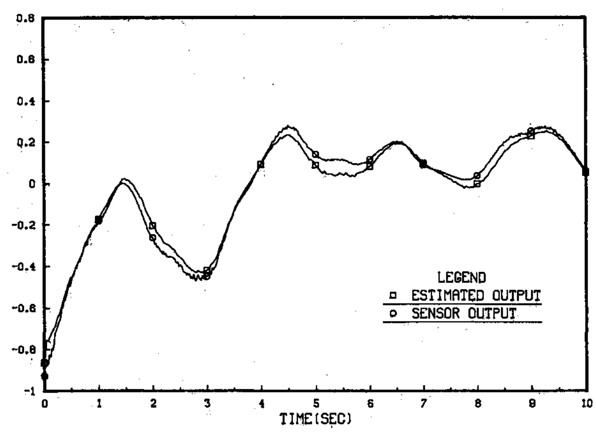

Fig. 6 Estimate of 8th sensor (9th sensor fails, no corrective action).

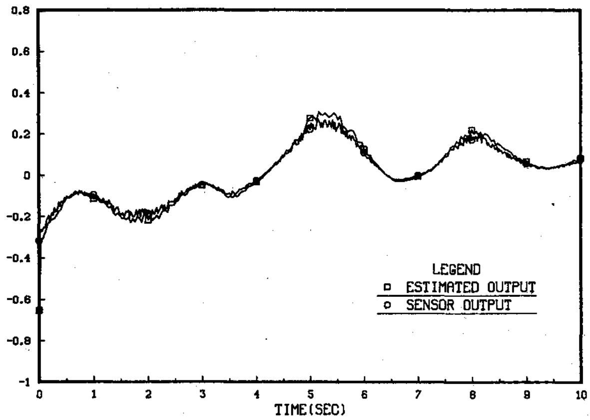

Fig. 7 Estimate of 9th sensor (9th sensor fails, no corrective action).

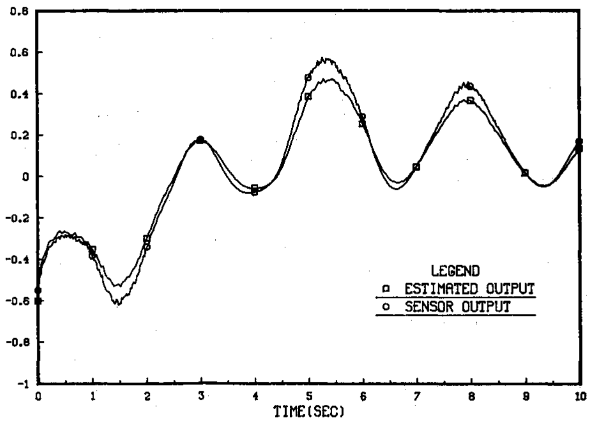

Fig. 8 Estimate of 10th sensor (9th sensor fails, no corrective action).

The sensors output is contaminated by random noise where the following model is assumed for the measurement noise. The actual sensor's output, denoted by $\dot{y}_{aj}(t)$ is taken as

$$\dot{y}_{aj}(t) = \dot{y}_j(t)[1+R], \qquad j=1,2,...,p \tag{42}$$

where $\dot{y}_j(t)$ is the actual velocity at the jth sensor, and R is a random variable with a uniform distribution in $[-0.03, 0.03]$. This model seems more realistic than using a Gaussian distribution, because the amount of measurement error is related to the actual velocity. In the event of failure, the range of R for the faulty sensor is taken as $[-0.06, 0.06]$.

First, we investigate the effects of sensor failure. Tables 1 and 2 compare the first eight columns of CD and CSD for the controlled modes (first four) when 11 sensors are used to implement the modal filters. CSD is computed when the fifth sensor fails by 50%, i.e., $S_5 = 0.5$. Ideally, i.e., when an adequate number of sensors are used and there is no failure, the first four columns of CD should approach an identity matrix, and the next columns should approach a null matrix.[19] Tables 3 and 4 compare CD and CSD for 13 sensors. As expected, the effects of sensor failure become less drastic when the number of sensors is increased, which is evident from the smaller off-diagonal terms in both CD and CSD.

Next, we identify failure of the 9th sensor ($j=9$). We assume that 11 modes contribute to the system response ($\ell = 11$), so that there are four unmodeled modes, which contaminate the identification results. A sensor failure mode is selected such that $S_9 = 0.5$, and failure occurs at $t=0$ s. A sampling period of $T=0.02$ s is chosen, which is adequate for small angle assumption. Before the identification (and the control) begins, the beam is excited for two seconds using a parabolic excitation of the form $f(x,t) = F_0 t(t+2)\delta(x-x_0)$, $-2 \le t \le 0$, where $x_0 = 6.7$, and $F_0 = 3$. The control force is applied for two sampling periods. Proportional damping of $\zeta_r = 0.02$ is added to each mode, which introduces parameter uncertainties into the identification process, because Eqs. (33) are based on an undamped model. For the cases when corrective action is not taken, the modal coordinates are extracted using the inverse of Eq. (19), so that the number of monitored modes is the same as the number of sensors.

In Figs. 1-4, the estimates of the 6th, 8th, 9th, and 10th sensors are plotted and compared with the actual sensor's measurements in the event of no failure. The estimation is based on Eq. (33a) and Eq. (35).

Figures 5-8 show the estimate of $\dot{y}_6(t)$, $\dot{y}_8(t)$, $\dot{y}_9(t)$, and $\dot{y}_{10}(t)$ in the event of failure of the 9th sensor by 50%. As can be seen, all estimates are affected. However, estimate of the 6th sensor is affected less. System simulations for failures of other sensors indicated that failure of a sensor affects estimates of nearby sensors more than sensors further apart,[23] which is to be expected.

We next consider identification of the faulty sensor. First we assume that the 9th sensor is faulty, and remove it from operation. To this end, we have two choices: the first is to estimate the 9th sensor's output by interpolation of nearby sensors. The second choice is to use Eq. (37). System simulations showed that the second approach gave more reliable results, even though 4 sensors were used in the interpolation.[23] This is because interpolation is a smoothing process and it eliminates contributions of the higher modes. When using Eq. (37), it was observed that identification of the faulty sensor becomes more effective if the output of the sensor to be estimated is removed from D as well. This implies that to estimate $\dot{y}_9(t)$ the ninth sensor is removed, but to estimate $\dot{y}_8(t)$ both the outputs $\dot{y}_8(t)$ and $\dot{y}_9(t)$ are removed. Figures 9-12 show the estimates of $\dot{y}_6(t)$, $\dot{y}_8(t)$, $\dot{y}_9(t)$, and $\dot{y}_{10}(t)$ us-

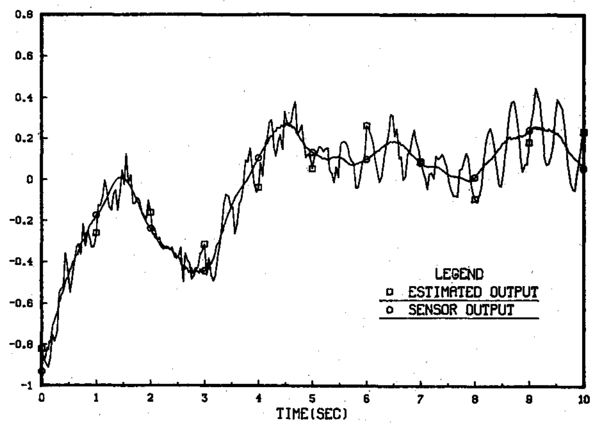

Fig. 10 Estimate of 8th sensor assuming that the 9th sensor is faulty.

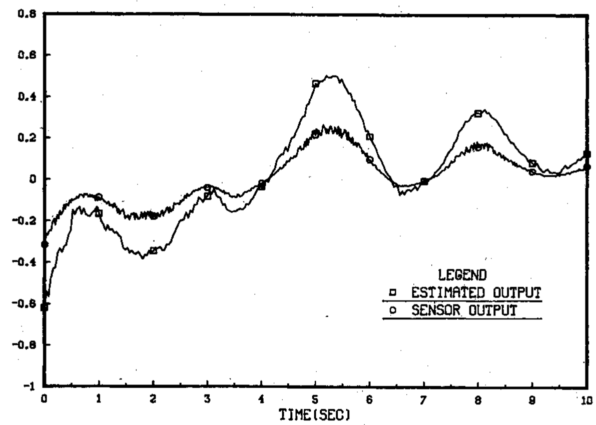

Fig. 11 Estimate of 9th sensor assuming that the 9th sensor is faulty.

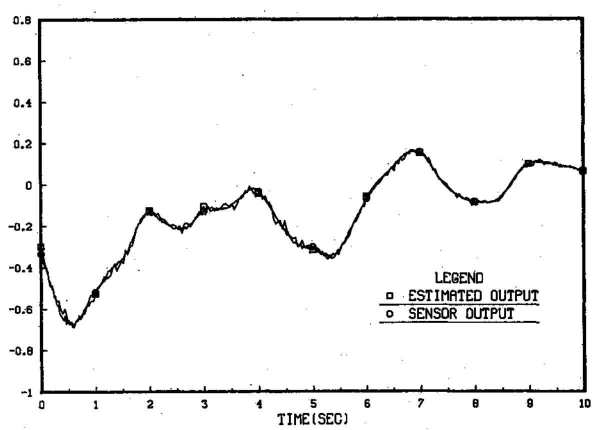

Fig. 9 Estimate of 6th sensor assuming that the 9th sensor is faulty.

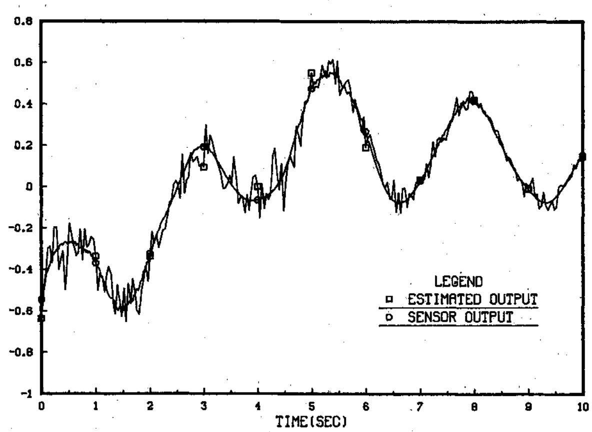

Fig. 12 Estimate of 10th sensor assuming that the 9th sensor is faulty.

Table 3 *CD* matrix for 13 sensors

1.0000	0.0000	0.0000	0.0000	0.0000	0.0000	0.0000	0.0000
0.0000	0.9993	0.0000	0.0000	0.0000	0.0000	0.0000	0.0000
0.0000	0.0000	0.9967	0.0000	0.0000	0.0000	0.0000	0.0000
0.0000	0.0000	0.0000	0.9900	0.0000	0.0000	0.0000	0.0000

Table 4 *CSD* matrix for 13 sensors

0.9909	−0.0163	−0.0203	−0.0203	−0.0163	−0.0091	0.0000	0.0091
−0.0168	0.9691	−0.0377	−0.0377	−0.0302	−0.0168	0.0000	0.0168
−0.0217	−0.0392	0.9479	−0.0489	−0.0392	−0.0217	0.0000	0.0217
−0.0227	−0.0409	−0.0510	0.9390	−0.0409	−0.0227	0.0000	0.0227

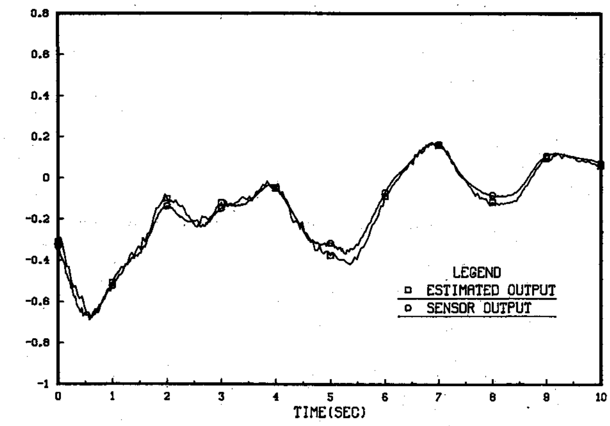

Fig. 13 Estimate of 6th sensor assuming that the 10th sensor is faulty.

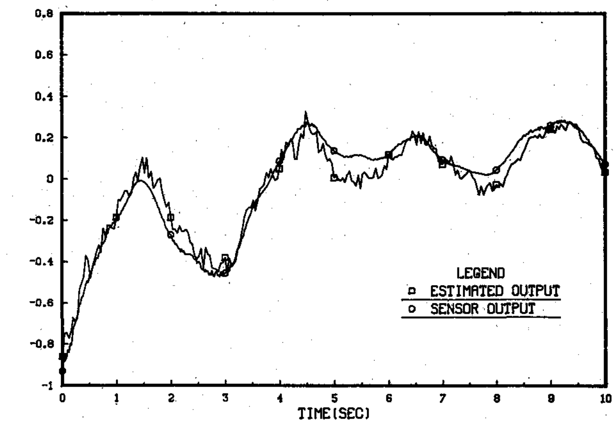

Fig. 14 Estimate of 8th sensor assuming that the 10th sensor is faulty.

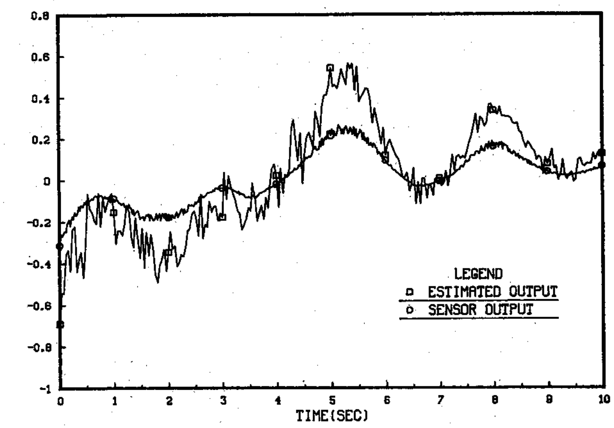

Fig. 15 Estimate of 9th sensor assuming that the 10th sensor is faulty.

ing this approach. We observe that the estimates $\hat{y}_6(t)$, $\hat{y}_8(t)$, and $\hat{y}_{10}(t)$ approach their actual values, whereas $\hat{y}_9(t)$ becomes even more different than in Fig. 7, leading to the conclusion that assuming the 9th sensor as faulty was correct.

Note that when corrective action is taken, because fewer numbers of sensors are used, the estimates of $\dot{y}_j(t)$ are more contaminated by the unmodeled modes, and the measurement noise is amplified. However, the nature of this contamination is known, as well as the rate at which the noise and higher mode participation is amplified, so that one can consider these effects when evaluating the quality of the estimate.[23]

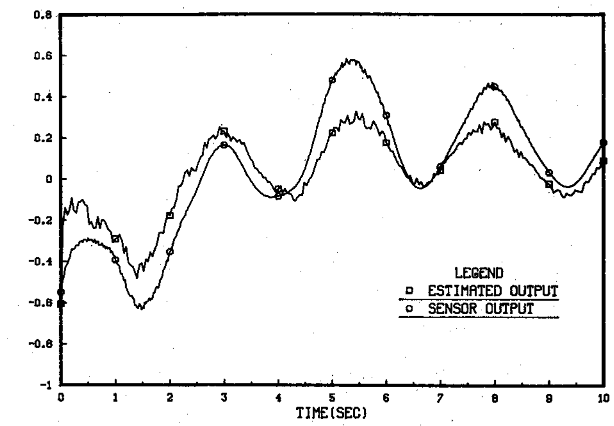

Fig. 16 Estimate of 10th sensor assuming that the 10th sensor is faulty.

Finally, we investigate the effects of suspecting an operational sensor of being faulty. Figures 13–16 plot the estimates of $\dot{y}_6(t)$, $\dot{y}_8(t)$, $\dot{y}_9(t)$, and $\dot{y}_{10}(t)$ when the 10th sensor is assumed to be faulty, and is removed from operation. Actually, from Figs. 5–8, the first logical choice would have been to suspect the 10th sensor as faulty. As can be seen, none of the estimates match their exact measurements, leading to the conclusion that assuming the 10th sensor as faulty was not correct. Considering the forementioned arguments, we observe that Fig. 10 is a better estimate of $\dot{y}_8(t)$ than Fig. 14 because the estimation error $[\dot{y}_8(t)-\hat{\dot{y}}_8(t)]$ has the form of a sinusoidal with varying amplitude and frequency of the 12th mode, which is not monitored. Comparison of other sensors outputs and estimates clearly indicate that the 10th sensor is an operational one.[23]

During implementation of the failure detection, plots of the system response need to be examined and compared continuously. The procedure has to be automated and performed by a digital computer. A method was developed by Choe[23] to identify a suspect sensor by examining the differences between the estimated amplitudes and sensors measurements. The detection criterion is based on the integral of the difference between the estimated and actual sensors output. On-line implementaion will require use of concepts from artificial intelligence.

Note that after the faulty component is identified, its estimate obtained by Eq. (37) or interpolation can be used until a spare sensor is brought online and the control system is reconfigured. It was observed during system simulations that having a larger number of sensors resulted in a more reliable failure detection by minimizing the effects of measurement noise, actuator noise, and observation spillover. By having additional sensors a more accurate knowledge about the system behavior can be given, thus leading to more reliable decisions regarding failure. It was also observed during system simulations that the failure detection becomes more diffficult if the level of failure is low. On the other hand, a very low level of failure may not have adverse effects and it may be tolerated, especially as larger numbers of sensors are used.

VII. Conclusions

A method is described for the detection of sensor failures in flexible structures. The method is applicable when a large number of components are used. Amplitudes of the system motion at the sensors locations are estimated. These estimates are then compared with the actual sensors measurements to detect failure and identify the faulty sensor. Because failure of a sensor affects failure detection in nearby sensors as well, a sequential decision-making scheme is proposed to improve the reliability of the failure detection. Increasing the number of sensors reduces the adverse effects of failure, and facilitates the failure detection process; however, it increases the probabilities of failure.

Acknowledgment

The work reported herein was supported by National Science Foundation Grant MSM 85-01877.

References

[1]Friedland, B., "Maximum Likelihood Failure Detection of Aircraft Flight Control Sensors," *Journal of Guidance, Control, and Dynamics,* Vol. 5, Sept.-Oct. 1982, pp. 498-503.

[2]Montgomery, R.C. and Price D.B., "Failure Accommodation in Digital Flight Control Systems Accounting for Nonlinear Aircraft Dynamics," *Journal of Aircraft,* Vol. 13, Feb. 1976, pp. 76-82.

[3]Wagdi, M.N., "An Adaptive Control Approach to Sensor Failure Detection and Isolation," AIAA Paper 82-0182, Jan. 1982.

[4]Erdle, F.E., Feigenbaum, I.A., and Talcott, J.W.Jr., "Reliability Programs for Commercial Communication Satellites," *IEEE Transactions on Reliability,* Vol. R-32, No. 3, 1983, pp. 236-239.

[5]Willsky, A.S., "A Survey of Design Methods for Failure Detection in Dynamic Systems," *Automatica,* Vol. 12, 1976, pp. 601-611.

[6]Deyst, J.J., Harrison, J.V. Jr., Gai, E., and Daly, K.C., "Fault Detection, Identification and Reconfiguration for Spacecraft Systems," *The Journal of the Astronautical Sciences,* Vol. 29, 1981, pp. 113-126.

[7]Chow, E.Y. and Willsky, A.S., "Issues in the Development of a General Design Algorithm for Reliable Failure Detection," *Proceedings of the 1980 Conference on Decision and Control,* IEEE, New York, Dec. 1980, pp. 1006-1012.

[8]Turpule, B.R. and Knapp, C.H., "Robust Detection and Estimating Soft Failures in Linear Systems," *Proceedings of the 1980 Conference on Decision and Control,* IEEE, New York, Dec. 1980, pp. 1013-1019.

[9]Leininger, G.G., "Model Degradation Effects on Sensor Failure Detection," 1981 Joint Automatic Control Conference, Charlottesville, VA, June 1981.

[10]Alexandro, F.J. and Tjov, J., "Instrument Failure Detection and Isolation in a System with Variable Plant Parameters," *Proceedings of the AIAA Guidance and Control Conference,* AIAA, New York, Aug. 1984, pp. 176-181.

[11]Clark, R.N. and Campbell, B., "Instrument Fault Detection in a Pressurized Water Reactor Pressurizer," *Nuclear Technology,* Vol. 56, 1982, pp. 23-32.

[12]VanderVelde, W.E., "Component Failure Detection in Flexible Spacecraft Control Systems," 4th Virginia Polytechnic Institute and State University/AIAA Symposium on Dynamics and Control of Large Flexible Structures," Blacksburg, VA, June 1983, pp. 481-497.

[13]VanderVelde, W.E. and Carignan, C.R., "Number and Placement of Control System Components Considering Possible Failures," *Journal of Guidance, Control, and Dynamics,* Vol. 7, 1984, pp. 703-709.

[14]Montgomery, R.C., "Reliability Considerations in the Placement of Control System Components," AIAA Paper 83-2260, Aug. 1983.

[15]Benhabib, R.J., Iwens, R.P., and Jackson, R.L., "Adaptive Control for Large Space Structures," 18th IEEE Conference on Decision and Control, Ft. Lauderdale, FL, Dec. 1978.

[16]Baruh, H., "Actuator Failure Detection in the Control of Distributed Systems," *Journal of Guidance, Control, and Dynamics,* Vol. 9, 1986, pp. 181-189.

[17]Meirovitch, L. and Baruh, H., "Control of Self-Adjoint Distributed-Parameter Systems," *Journal of Guidance, Control, and Dynamics,* Vol. 5, 1982, pp. 60-66.

[18]Balas, M.J., "Active Control of Flexible Systems," *Journal of Optimization Theory and Applications,* Vol. 25, No. 3, 1978, pp. 415-436.

[19]Meirovitch, L. and Baruh, H., "On the Implementation of Modal Filters for Control of Structures," *Journal of Guidance, Control, and Dynamics,* Vol. 8, Nov.-Dec. 1986, pp. 707-716.

[20]Aubrun, J.N., "Theory of the Control of Structures by Low-Authority Controllers," *Journal of Guidance and Control,* Vol. 3, Sept.-Oct. 1980, pp. 444-451.

[21]Ahlberg, J.H., Nilson, E.N. and Walsh, J.L., *The Theory of Splines and Their Applications,* Academic Press, New York, 1967.

[22]Baruh, H. and Silverberg, L.M., "Natural Robust Control of Distributed Systems," *Journal of Guidance, Control, and Dynamics,* Vol. 8, Nov.-Dec. 1985, pp. 717-724.

[23]Choe, K., "Modeling and Sensor Failure Detection in Flexible Structures," M.S. Thesis, Rutgers University, New Brunswick, NJ, May 1987.